

SDSS J083253.18+064316.7: one strange object with double-peaked narrow $H\alpha$ but single-peaked narrow $H\beta$

Xue-Guang Zhang^{1,2*}

¹*Purple Mountain Observatory, Chinese Academy of Sciences, 2 Beijing XiLu, NanJing, JiangSu, 210008, P. R. China*

²*Chinese Center for Antarctic Astronomy, NanJing, JiangSu, 210008, P. R. China*

ABSTRACT

In this letter, we firstly report one unique object SDSS J0832+0643 with particular features of narrow balmer emission lines: double-peaked narrow $H\alpha$ but single-peaked narrow $H\beta$. The particular features can not be expected by currently proposed kinematic models for double-peaked narrow emission lines, because the proposed kinematic models lead to similar line profiles of narrow balmer emission lines. However, due to radiative transfer effects, the non-kinematic model can be naturally applied to well explain the particular features of narrow balmer emission lines: larger optical depth in $H\alpha$ than 10 leads to observed double-peaked narrow $H\alpha$, but smaller optical depth in $H\beta$ around 2 leads to observed single-peaked narrow $H\beta$. Therefore, SDSS J0832+0643 can be used as strong evidence to support the non-kinematic model for double-peaked narrow emission lines.

Key words: Galaxies:Active – Galaxies:nuclei – Galaxies:Seyfert – quasars:Emission lines

1 INTRODUCTION

Dual supermassive black holes could be one inevitable stage, if co-evolution of supermassive black holes and host galaxies was accepted (Silk & Rees 1998, Di Matteo, Springel & Hernquist 2005, Hopkins et al. 2006). Once separations of central two supermassive black holes are around kilopcs scale, double-peaked narrow emission lines could be expected, if there are significant velocities along the line-of-sight of the dual supermassive black holes. Therefore, double-peaked narrow emission lines can be treated as one indicator of candidate dual supermassive black holes with separations about kilo-pcs, such as the following reported well studied candidates among AGNs with double-peaked narrow emission lines, SDSS J1048 (Zhou et al. 2004) DEEP2 J1420+5259 (Gerke et al. 2007), EGSD2 J1415 (Comerford et al. 2009a), COSMOS J1000 (Comerford et al. 2009, Blecha et al. 2013, Wrobel, Comerford & Middelberg 2014), SDSS J1316 (Xu & Komossa 2009), SDSS J1517 (Rosario et al. 2010), SDSS J1715 (Comerford et al. 2011), SDSS J1502 (Fu et al. 2011b), SDSS J0952 (Mcgurk et al. 2011), SDSS J1426 (Barrows et al. 2012), SDSS J1502 (Fu et al. 2012), 3C316 (An et al. 2013), NDWFS J1432 and J1433 (Comerford et al. 2013), SDSS J1108, J1146, J1131 and J1332 (Liu et al. 2013), SDSS J1323 (Woo et al. 2014), etc.. And then, some samples of objects with double-peaked narrow emission lines are reported as candidates for objects

with dual supermassive black holes, such as Wang et al. (2009), Smith et al. (2010) and Ge et al. (2012) etc..

Besides the dual supermassive black holes, there are another kinematic models which can be applied to explain observed double-peaked narrow emission lines, such as radial outflows and rotating disk systems (Liu et al. 2010, Fischer et al. 2011, Shen et al. 2011, Comerford et al. 2012, Fischer et al. 2013, etc.). Through high-quality NIR images discussed in Fu et al. (2011) for 50 double-peaked narrow line AGNs, in Shen et al. (2011) for 31 double-peaked narrow line AGNs and in Fu et al. (2012) for 42 double-peaked narrow line AGNs, one conclusion has been reported that among their small sample of double-peaked narrow line AGNs, scenarios involving a single AGN can produce double-peaked narrow emission lines with considerations of gas kinematics for large part of the double-peaked narrow line AGNs, only a small part of double-peaked narrow line AGNs probably contain dual supermassive black holes.

Furthermore, besides the proposed kinematic models for double-peaked narrow emission lines, there is one another non-kinematic model, the model based on radiative transfer effects in optically thick sources (more recent detailed discussions on the non-kinematic model can be found in Elitzur, Ramos & Ceccarelli 2012), which can also be well applied to explain observed double-peaked narrow emission lines. And moreover, as what have been discussed in literature, it is generally impossible to disentangle the effects of kinematics and line opacities in observed double-peaked emission lines.

However, we should note that there are some different

* xgzhang@pmo.ac.cn

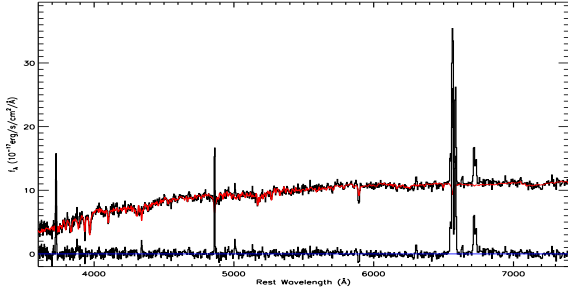


Figure 1. SDSS spectrum and line spectrum of SDSS J0832+0643. From top to bottom, solid line in black shows the SDSS spectrum, solid line in red shows the determined stellar contributions, solid line in black shows the pure line spectrum, and solid line in blue shows $f_{\lambda} = 0$. Here, in order to show more clearer plots, the observed spectrum and the line spectrum are smoothed by average values per 4 data points.

model expected features of double-peaked narrow emission lines, based on proposed kinematic and non-kinematic models. On the one hand, the kinematical models should lead to the similar line profiles of double-peaked narrow balmer emission lines, because the kinematic models have the same effects on narrow balmer emission lines. On the other hand, due to much different line opacities for narrow balmer emission lines, the non-kinematic model could lead to some different double-peaked narrow balmer emission lines. However, in the literature, there are so far no reliable results reported on non-kinematic origin of double-peaked narrow emission lines. Here, in this letter, we firstly report such a unique object with double-peaked narrow H α but single-peaked narrow H β , which will provide strong evidence to support the non-kinematic model leading to the different line profiles of narrow balmer emission lines. In section 2, we give our main results and discussions on the object SDSS J0832+0643. And in section 3, we give our final conclusions.

2 MAIN RESULTS

In order to check properties of broad balmer emission lines of double-peaked narrow line AGNs, emission lines have been carefully checked for all the double-peaked narrow line objects reported in Ge et al. (2012), which will provide further information on origin of double-peaked narrow emission lines (Zhang 2015, submitted to MNRAS). When we check shifted velocities of broad balmer lines relative to double-peaked narrow balmer lines, we find SDSS J083253.18+064316.7 (=SDSS J0832+0643) with the single-peaked narrow H β . Except the SDSS J0832+0643, no other objects can be found with so strange narrow balmer lines. Then, by the following fitted results for narrow balmer emission lines and the following Kolmogorov-Smirnov statistic results, we can confirm that it is true for double-peaked narrow H α but single-peaked narrow H β .

The observed SDSS spectrum is shown in Figure 1 for SDSS J0832+0643. In order to show more clearer properties of narrow balmer emission lines, the stellar lights in the spectrum should be firstly subtracted. Here, the more recent proposed pPXF method (Penalized Pixel-Fitting method discussed in Cappellar & Emsellem 2004) with 224

MILES (Medium resolution INT Library of Empirical Spectra, Vazdekis et al. 2012) template spectra is applied to determine the stellar contributions, because the regularization technique included in the pPXF method could lead to more smoother solutions on spectral decomposition. Here, The 224 MILES template spectra have stellar ages from 0.0631Gyr to 17.7828Gyr and have $[M/H]$ from -2.32 to 0.22. The determined stellar contributions by the pPXF method are shown in Figure 1.

Based on the pPXF determined results, the stellar velocity dispersion of host galaxy is about 155 ± 17 km/s in SDSS J0832+0643, which is consistent with the reported value 158 ± 15 km/s determined by the STARLIGHT code (Cid Fernandes et al. 2005) in Ge et al. (2012). The coincident results indicate our determined stellar components are reliable. Then, after stellar lights being removed, emission lines can be well checked. And we can find that SDSS J0832+0643 is one type 2 objects with pure narrow emission lines: strong narrow balmer lines and much weak $[O III]\lambda 5007\text{\AA}$ line. Figure 2 shows the fitted results for narrow emission lines by gaussian functions. In this paper, we mainly focus on the lines of narrow H α , narrow H β and $[N I]\lambda 6548, 6583\text{\AA}$ doublet. The determined line parameters are listed in Table 1. Here, there is one important point we should note. When our procedure is applied to describe each narrow emission line by two gaussian functions, we try to fit the narrow H β by the similar line profile of the double-peaked narrow H α . However, we find that FWHM (full width at half maximum) is about 510 km/s for the narrow H α , but is only 270 km/s for the narrow H β . The much different FWHMs strongly indicate different line profiles of narrow balmer lines. So that the narrow H β is fitted without considerations of line profile of double-peaked narrow H α . Furthermore, although two gaussian components are applied to fit the narrow H β in our procedure, the fitted result for narrow H β leads to zero flux of one component, which indicates one gaussian function is good enough to describe the narrow H β . Furthermore, the two-sided Kolmogorov-Smirnov statistic technique is applied to check difference between line profiles of narrow balmer lines. Based on the line profile of narrow H β from the observed spectrum with stellar contributions being subtracted and the line profile of narrow H α created by the two gaussian components listed in Table 1, the Kolmogorov-Smirnov statistic gives one probability about 0.0015 to support the assumption that narrow H α and narrow H β have the similar line profile. And moreover, based on the line profile of narrow H β from the observed spectrum with stellar contributions being subtracted and the fitted result for the narrow H β by the one gaussian components listed in Table 1, the Kolmogorov-Smirnov statistic gives one probability about 83% to support the assumption that the narrow H β has one gaussian line profile. Therefore, one gaussian function rather than two gaussian functions is preferred to describe the narrow H β .

Before proceeding further, simple comparisons are shown with reported results of double-peaked narrow H α in Ge et al. (2012) for SDSS J0832+0643. In Ge et al. (2012), the reported line parameters of the double-peaked narrow H α are as follows: $\sigma \sim 2.2 \pm 0.1\text{\AA}$ and $flux \sim 145.8 \pm 10.5 \times 10^{-17} \text{ erg/s/cm}^2$ for the blue component, and $\sigma \sim 2.6 \pm 0.1\text{\AA}$ and $flux \sim 210.4 \pm 11.9 \times 10^{-17} \text{ erg/s/cm}^2$ for the red component respectively. It is clear that the results

Table 1. Line parameters

line	mark	λ_0	σ	flux
H α	blue	6560.3 \pm 0.13	2.1 \pm 0.1	128 \pm 8
	red	6566.3 \pm 0.13	2.6 \pm 0.1	201 \pm 9
[N II]	blue	6580.9 \pm 0.13	2.4 \pm 0.1	73 \pm 5
	red	6586.9 \pm 0.13	2.7 \pm 0.1	102 \pm 5
H β		4861.8 \pm 0.2	1.9 \pm 0.2	66 \pm 9

Notice: The first column shows which line is measured, the second column shows which component of the line is measured. The third column shows the center wavelength in unit of \AA for the component, the fourth column shows the second moment in unit of \AA for the component and the fifth column shows the flux in unit of $10^{-17} \text{erg/s/cm}^2$ of the component.

on line width and line flux listed in Table 1 are well consistent with reported results in Ge et al. (2012). And moreover, the peak separation is about $5.99 \pm 0.26 \text{\AA}$ in Ge et al. (2012), which is also well consistent with our result $6 \pm 0.26 \text{\AA}$. The results indicate our determined line parameters of double-peaked narrow H α are reliable. Furthermore, there is one point we should note. In Ge et al. (2012), when emission lines were determined, there was one strong criterion that each narrow emission line had the similar double-peaked line profile, which led to mathematic determined line parameters of two fake components of narrow [O III] $\lambda 5007 \text{\AA}$ and narrow H β of SDSS J0832+0643, and then led to classification of one two Type 2 AGNs of SDSS J0832+0643. However, it is clear that there are much different line profiles of narrow balmer lines, which indicate the criterion applied in Ge et al. (2012) is not valid for the narrow balmer lines of SDSS J0832++0643. So that, in this paper, we do not show further discussions on classification of SDSS J0832++0643. Based on the results discussed above, we can find that the narrow H α is double-peaked but the narrow H β is single-peaked in SDSS J0832+0643. This is so far the only one reported unique object with the double-peaked narrow H α but the single-peaked narrow H β . And moreover, the single-peaked narrow H β is not corresponding to blue or red component of the double-peaked narrow H α , through their determined center wavelengths listed in Table 1. Then, we can check the theoretical models for the particular features of narrow balmer emission lines.

Under the kinematic models for double-peaked narrow emission lines, there is no way to expect so different line profiles of narrow balmer emission lines. Even, with considerations of uncertainties, we could assume that the single-peaked narrow H β could be related to the red component of double-peaked narrow H α . It looks that the dual supermassive black holes could be applied to explain the observed features of narrow balmer lines with disappearance of the blue component of the narrow H β , if there was much larger dust extinction for the blue components of the intrinsic double-peaked narrow balmer emission lines. Under the assumed case with large dust extinction for the blue components, we would expect the $E(B - V)$ could be not less than 1 (flux ratio of H α to H β larger than 10). However, for the red components of double-peaked narrow balmer lines, the flux ratio of H α to H β is only 3.05, one common standard value. If the dust extinction in the blue component was due to

abundant dusts due to galaxy merging, it is natural to expect that there should be similar effects of merging on the two components. If we assume that the single-peaked narrow H β could be related to the blue component of double-peaked narrow H α , similar results can be found: flux ratio of the red components of narrow H α to narrow H β is larger than 10, but the flux ratio of the blue component is only 1.9. Therefore, the dual supermassive black holes could not be one natural choice to explain the observed features of double-peaked narrow H α but single-peaked narrow H β of SDSS J0832+0643.

The non-kinematic model can be one natural and reasonable model to explain double-peaked narrow H α but single-peaked narrow H β . Based on the measured line flux of total H α to H β , the flux ratio is about 5, which indicate the optical depths in H α and in H β are about $\tau_{H\alpha} \sim 10 - 11$ and $\tau_{H\beta} \sim 0.2 \times \tau_{H\alpha} \sim 2$ respectively, with the following assumptions of optical depth of Ly α about 10^{5-6} and electron density $N_e \sim 10^8 \text{cm}^{-3}$ as discussed in Luna & Costa (2005). Here, we do not have enough information to give one reliable estimation on electron density. But $N_e \sim 10^8 \text{cm}^{-3}$ could be accepted, such as the listed lower limit values of electron densities for southern symbiotic stars in Luna & Costa (2005). And moreover, the very weak [O III] $\lambda 5007 \text{\AA}$ line support the high electron density to some extent. Furthermore, Figure 3 shows the SDSS image of SDSS J0832+0643: one clear merging system. Therefore, there could be abundant dusts in central region of SDSS J0832+0643, which can naturally explain the large flux ratio of narrow H α to narrow H β .

Once, the optical depths in H α and in H β are simply determined, we can give some discussions on different line profiles of narrow balmer emission lines. As more recent discussions in Elitzur, Ramos & Ceccarelli (2012), optical depth around 10 can be treated as one boundary value: optical depth larger than 10 would lead to double-peaked narrow lines, but optical depth around 1 should not lead to double-peaked narrow lines. In SDSS J0832+0643, $\tau_{H\alpha} > 10$ but $\tau_{H\beta} \sim 2$ could lead to the double-peaked narrow H α but the single-peaked narrow H β . Furthermore, under the non-kinematic model, the peak separation (about 270km/s) of the two peaks of narrow H α can be described as $\sim 2 \times \nu_D \times \sqrt{\ln(\tau_{H\alpha})}$, where ν_D represents the broadening velocity due to the thermal motions. Therefore, $\nu_D \sim 80 - 90 \text{km/s}$ is enough to create the double-peaked narrow H α without contributions from rotating component, which indicates the electron temperature is about $10^5 - 10^6 \text{K}$. The expected ν_D leads to the expected peak separation of intrinsic double-peaked narrow H β is only 120km/s, therefore, it is hard to find apparent double-peaked features of narrow H β because of smaller peak separation. It is clear that the non-kinematic model with considerations of radiative transfer effects can be applied to well explain the observed double-peaked narrow H α but the single-peaked narrow H β in SDSS J0832+0643.

Before the end of the section, there are three points we should note. First and foremost, the non-kinematic model expected double-peaked narrow emission line could be symmetric to some extent. However, the observed double-peaked narrow H α of SDSS J0832+0643 is asymmetric to some extent, the red component is more stronger than the blue component. The asymmetric double-peaked narrow H α indicates

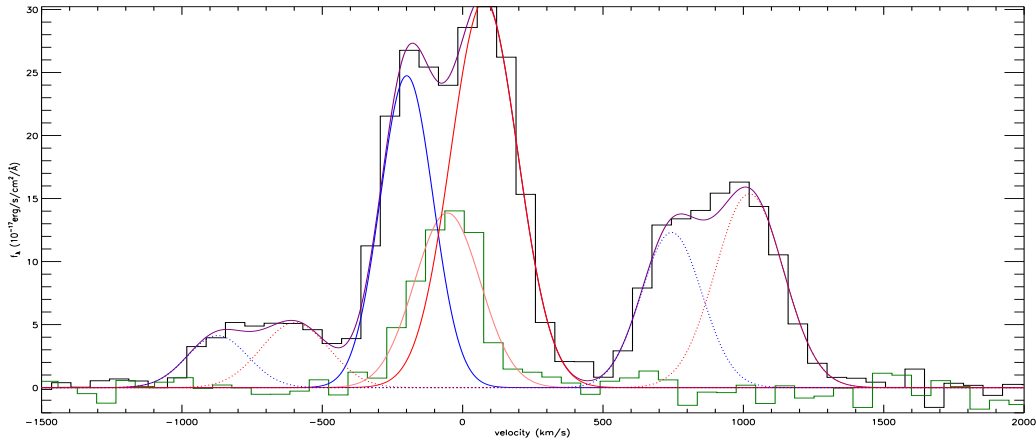


Figure 2. properties of narrow balmer emission lines in the velocity space. Solid line in black shows the line spectrum (stellar contributions having been subtracted) around $H\alpha$ (velocities calculated relative to center wavelength of 6564.61\AA). Solid line in purple shows the best fitted result by six narrow gaussian functions for the double-peaked narrow $H\alpha$ and the double-peaked $[\text{N II}]$ doublet. Solid lines in blue and in red show the blue component and the red component of the double-peaked narrow $H\alpha$ respectively. Dotted lines in blue and in red show the blue components and the red components of the double-peaked $[\text{N II}]$ doublet. Solid line in dark green shows the observed single-peaked narrow $H\beta$ in the velocity space (velocities calculated relative to center wavelength of 4862.68\AA), and thick solid line in pink represents the best fitted result for the narrow $H\beta$ by one gaussian function.

another weak component included in the narrow emission lines, one probable radial flow component. If the radial components were removed, the flux ratio of $H\alpha$ to $H\beta$ should be a bit larger than 5, leading to a bit larger $\tau_{H\alpha}$ leading to more consistent results with the observed features of narrow balmer lines.

Besides, it is hard to find the non-kinematic model expected double-peaked narrow emission lines, because much lower electron density in common NLRs leading to flux ratio of narrow $H\alpha$ to narrow $H\beta$ around 3 and smaller electron temperate leading to much smaller peak separations of expected double-peaked narrow emission lines.

Last but not least, we give further discussions to confirm that the narrow $H\alpha$ and the narrow $H\beta$ have much different line profiles. Figure 4 shows the line profiles of narrow balmer lines, before and after subtractions of stellar contributions. It is clear that even in the SDSS spectrum without subtractions of stellar contributions, there are double-peaked narrow $H\alpha$, but single-peaked narrow $H\beta$. And moreover, we have shown that the stellar velocity dispersion is about 155km/s (about 2.5\AA around $H\beta$), which is larger than the measured line width of narrow $H\beta$. Therefore, there are few effects of subtractions of stellar contributions on the single-peaked narrow $H\beta$, and the conclusion is reliable that the double-peaked narrow $H\alpha$ and the single-peaked narrow $H\beta$ are not fake.

3 CONCLUSIONS

Finally, we give our conclusions as follows. First and foremost, SDSS J0832+0643 is so far the firstly reported object with particular features of narrow balmer emission lines: double-peaked narrow $H\alpha$ but single-peaked narrow $H\beta$. Besides, the kinematic models can not explain the observed features of narrow balmer emission lines of SDSS J0832+0643. Last but not least, the non-kinematic model with considerations of radiative transfer effects can be applied to well ex-

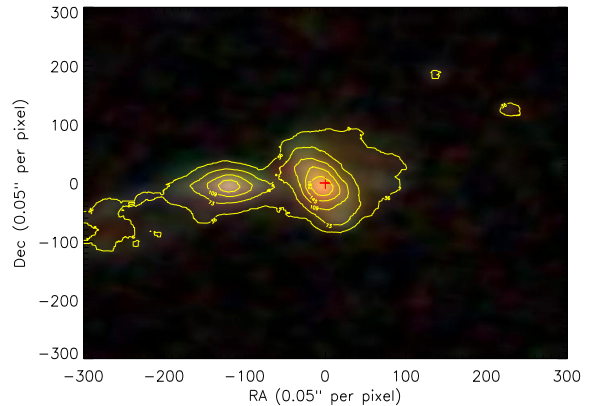


Figure 3. SDSS image of SDSS J0832+0643. Red plus shows the position with RA of 08:32:53.18 and DEC of +06:43:16.7, and each pixel in the image has a width of 0.05 arcseconds.

plain the observed features of narrow balmer emission lines of SDSS J0832+0643.

ACKNOWLEDGMENTS

Zhang X. G. gratefully acknowledge the anonymous referee for giving us constructive comments and suggestions to greatly improve our paper. Zhang acknowledges the kind support from the Chinese grant NSFC-11003043 and NSFC-11178003. This paper has made use of the data from the SDSS projects. SDSS-IV is managed by the Astrophysical Research Consortium for the Participating Institutions of the SDSS Collaboration including the Carnegie Institution for Science, Carnegie Mellon University, the Chilean Participation Group, Harvard-Smithsonian Center for Astrophysics, Instituto de Astrofísica de Canarias, The Johns

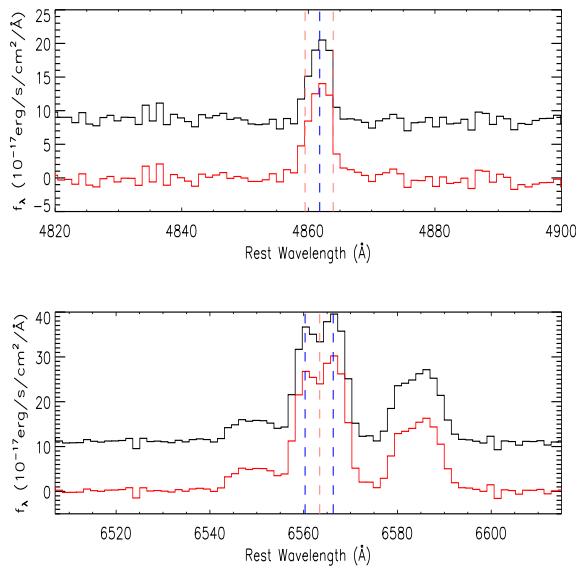


Figure 4. Properties of narrow H α (bottom panel) and narrow H β (top panel). In each panel, solid line in black shows the spectrum before subtractions of stellar contributions, and solid line in red shows the spectrum after subtractions of stellar contributions. The vertical dotted blue lines represent peak positions of the narrow balmer lines, 4861.8Å for the single-peaked narrow H β , and 6560.3Å and 6566.3Å for the double-peaked narrow H α . In top panel, the vertical pink dashed lines show expected peak positions ($[6560.3\text{Å}, 6566.3\text{Å}] \times 4862.68/6564.61$) based on the two peaks of the narrow H α . In bottom panel, the vertical pink dashed line shows expected peak position ($4861.8\text{Å} \times 6564.61/4862.68$) based on the peak of the narrow H β .

Hopkins University, Kavli Institute for the Physics and Mathematics of the Universe (IPMU) / University of Tokyo, Lawrence Berkeley National Laboratory, Leibniz Institut für Astrophysik Potsdam (AIP), Max-Planck-Institut für Astrophysik (MPA Garching), Max-Planck-Institut für Extraterrestrische Physik (MPE), Max-Planck-Institut für Astronomie (MPIA Heidelberg), National Astronomical Observatory of China, New Mexico State University, New York University, The Ohio State University, Pennsylvania State University, Shanghai Astronomical Observatory, United Kingdom Participation Group, Universidad Nacional Autónoma de México, University of Arizona, University of Colorado Boulder, University of Portsmouth, University of Utah, University of Washington, University of Wisconsin, Vanderbilt University, and Yale University.

REFERENCES

- An T., Paragi Z., Frey S., Xiao T., Bann W. A., et al., 2013, *MNRAS*, 433, 1161
- Barrows R. S., Stern D., Madsen K., Harrison F., Assef R. J., et al., 2012, *ApJ*, 744, 7
- Blecha L., Civano F., Elvis M., Loeb A., 2013, *MNRAS*, 428, 1341
- Cappellari, M. & Emsellem, E., 2004, *PASP*, 116, 138
- Cid Fernandes, R., Mateus, A., Sodre, L., Stasinska, G., Gomes, J. M., 2005a, *MNRAS*, 358, 363
- Comerford, J. M., Gerke, B. F., Newman, J. A., Davis, M., et al., 2009a, *ApJ*, 698, 956
- Comerford J. M., Griffith R. L., Gerke B. F., Cooper M. C., et al., 2009, *ApJL*, 702, 82
- Comerford J. M., Pooley D., Gerke B. F., Madejski G. M., 2011, *ApJL*, 737, 19
- Comerford J. M., Gerke B. F., Stern, D., Cooper, M. C., Weiner, B., et al., 2012, *ApJ*, 753, 42
- Comerford J. M., Schluns K., Greene J. E., Cool R. J., 2013, *ApJ*, 777, 64
- Di Matteo T., Springel V., Hernquist L., 2005, *Nature*, 433, 604
- Elitzur M., Ramos A. A., Ceccarelli C., 2012, *MNRAS*, 422, 1394
- Fischer, T. C., Crenshaw, D. M., Kraemer, S. B. et al. 2011, *ApJ*, 727, 71
- Fischer, T. C.; Crenshaw, D. M.; Kraemer, S. B.; Schmitt, H. R., 2013, *ApJS*, 209, 1
- Fu H., Myers A. D., Djorgovski S. G., Yan L., 2011, *ApJ*, 733, 103
- Fu H., Zhang X. Y., Assef R., Stockton A., Myers A. D., Yan L., Djorgovski S. G., Wrobel J. M., Riechers D. A., 2011b, *ApJL*, 740, 44
- Fu H., Yan L., Myers A. D., Stockton A., Djorgovski S. G., Rich J. A., 2012, *ApJ*, 745, 67
- Ge J. Q., Hu C., Wang J. M., Bai J. M., Zhang S., 2012, *ApJS*, 201, 31
- Gerke B. F., Newman J. A., Lotz J., Yan R. B., Barmby P., et al., 2007, *ApJL*, 660, 23
- Hopkins P. F., Hernquist L., Cox T. J., Di Matteo T., Robertson B., Springel V., 2006, *ApJS*, 163, 1
- Liu, X., Greene, J. E., Shen, Y., Strauss, M. A., 2010, *ApJ*, 715, L30
- Liu X., Civano F., Shen Y., Green P., Greene J. E., Strauss M. A., 2013, *ApJ*, 762, 110
- Luna G. J. M., & Costa R. D. D., 2005, *A&A*, 435, 1087
- Megurk R. C., Max C. E., Rosario D. J., Shields G. A., Smith K. L., Wright S. A., 2011, *ApJL*, 738, 2
- Rosario D. J., Shields G. A., Taylor G. B., Salviander S., Smith K. L., 2010, *ApJ*, 716, 131
- Shen Y., Liu X., Greene J. E., Strauss M. A., 2011, *ApJ*, 735, 48
- Silk J. & Rees M. J., 1998, *A&A*, 331, 1
- Smith K. L., Shields G. A., Bonning E. W., McMullen C. C., Rosario D. J., Salviander S., 2010, *ApJ*, 716, 866
- Vazdekis, A., Ricciardelli E., Cenarro, A. J., Diaz-Garcia, L.A., Falcon-Barroso, J., 2012, *MNRAS*, 424, 157
- Wang J. M., Chen Y. M., Hu C., Mao W. M., Zhang S., Bian W. H., 2009, *ApJL*, 705, 76
- Woo J. H., Cho H. J., Husemann B., Komossa S., Park D., Bennert V. N., 2014, *MNRAS*, 437, 32
- Wrobel J. M., Comerford J. M., Middelberg E., 2014, *ApJ*, 782, 116
- Xu, D. & Komossa, S. 2009, *ApJL*, 705, 20
- Zhou H. Y., Wang T. G., Zhang X. G., Dong X. B., Li C., 2004, *ApL*, 604, 33